Supporting Information

Programmable Peptide-Directed Two Dimensional Arrays of Various Nanoparticles on Graphene Sheets

Bong Gill Choi, MinHo Yang, Tae Jung Park, Yun Suk Huh, Sang Yup Lee, Won Hi Hong,* and HoSeok Park*

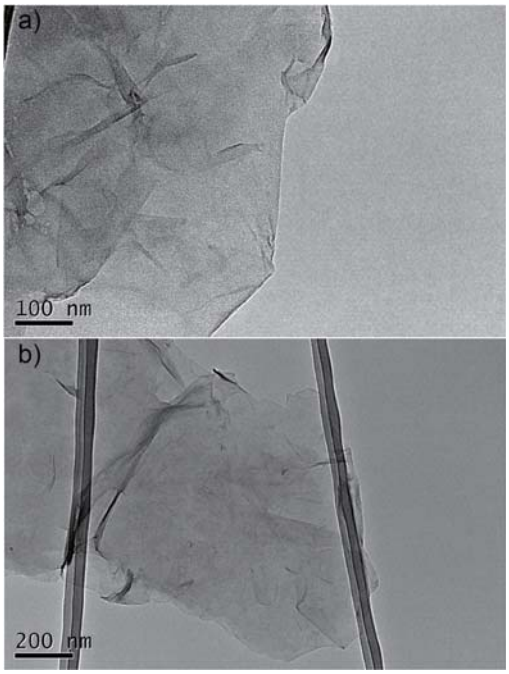

Fig. S1 TEM images of (a) GOP and (b) RGOP hybrids.

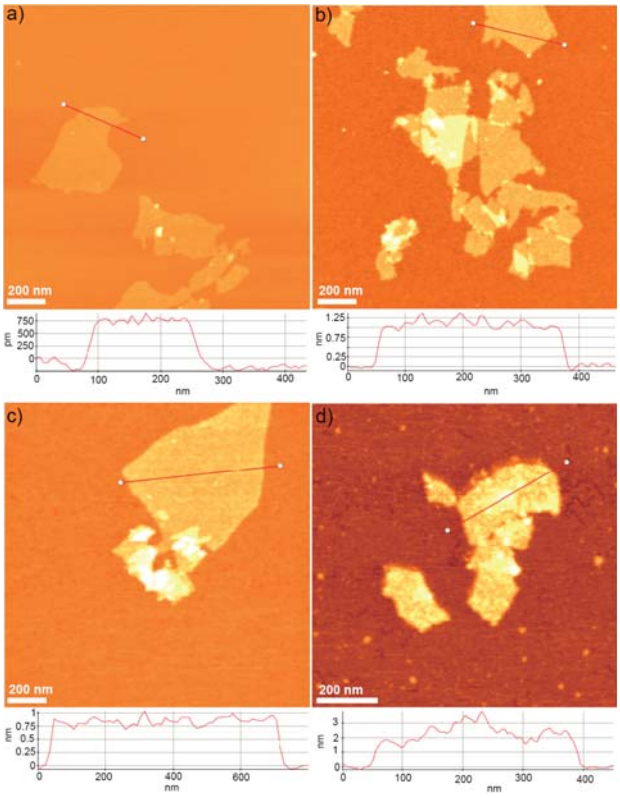

Fig. S2 AFM images of (a) GO, (b) GOP, (c) RGOP, and (d) RGOP-Pt hybrids.

Fig. S3 Photograph of RGOP-Pt hybrids in DI water.

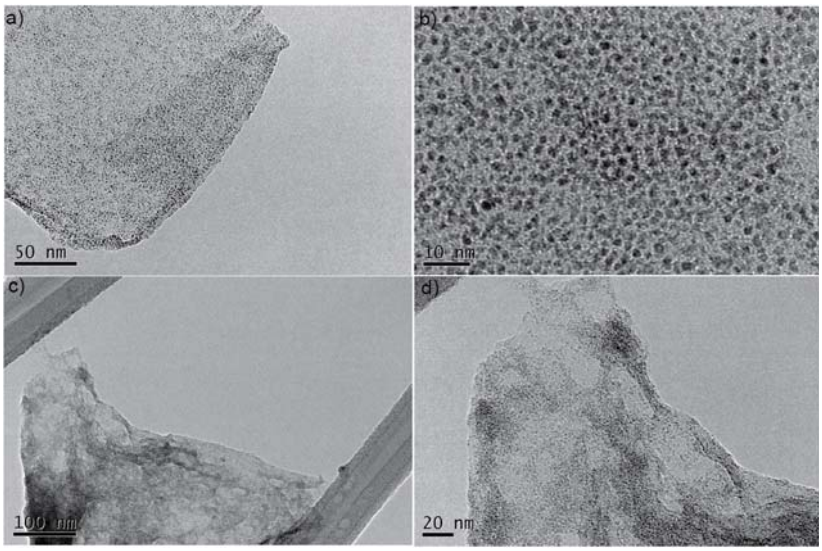

Fig. S4 (a) and (b) TEM images of RGOP- Pt hybrids with increasing sonochemical synthetic time of 20 min. (c) and (d) TEM images of RGOP-Pt hybrids with increasing metal salt concentration (4×10^{-3} mmol).

5

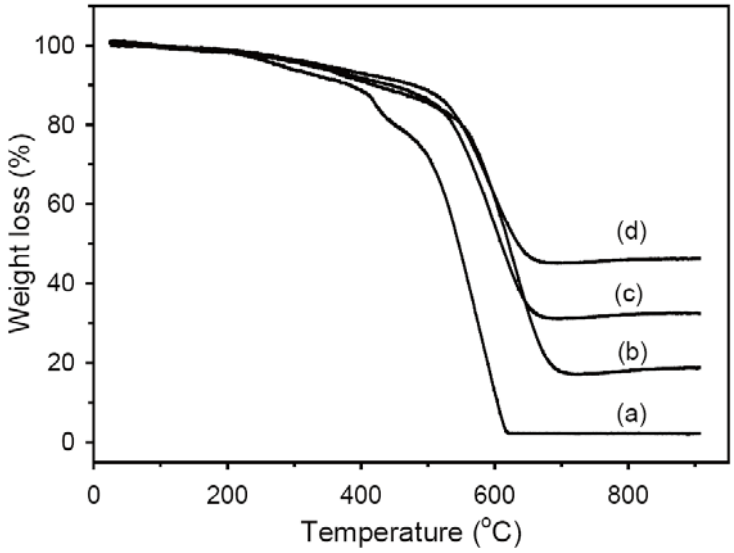

Fig. S5 TGA curves of (a) RGOP, (b) RGO-Pt, (c) and (d) RGOP-Pt hybrids with different metal salt concentration ((c) for 1×10^{-3} mmol of Pt precursor salt and (d) for 4×10^{-3} mmol of Pt precursor salt).

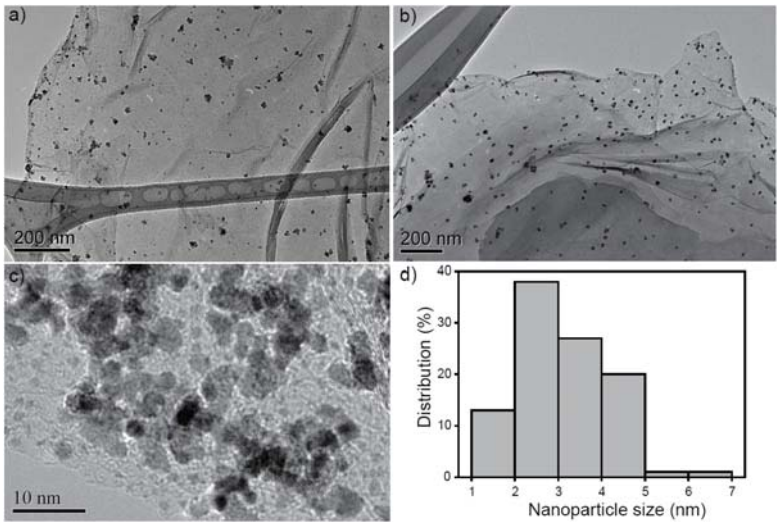

Fig. S6 TEM images of (a), (b), and (c) RGO-Pt hybrids and (d) size distribution of RGO-Pt hybrids.

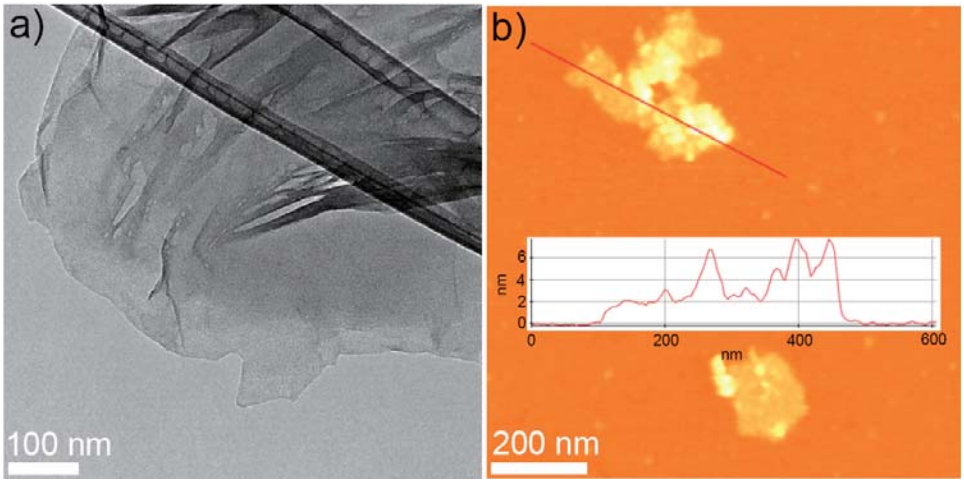

Fig. S7 (a) TEM image and (b) AFM image of RGOP hybrids with using $(E\text{-}G\text{-}G)_3\text{-}G$ of peptide sequences.

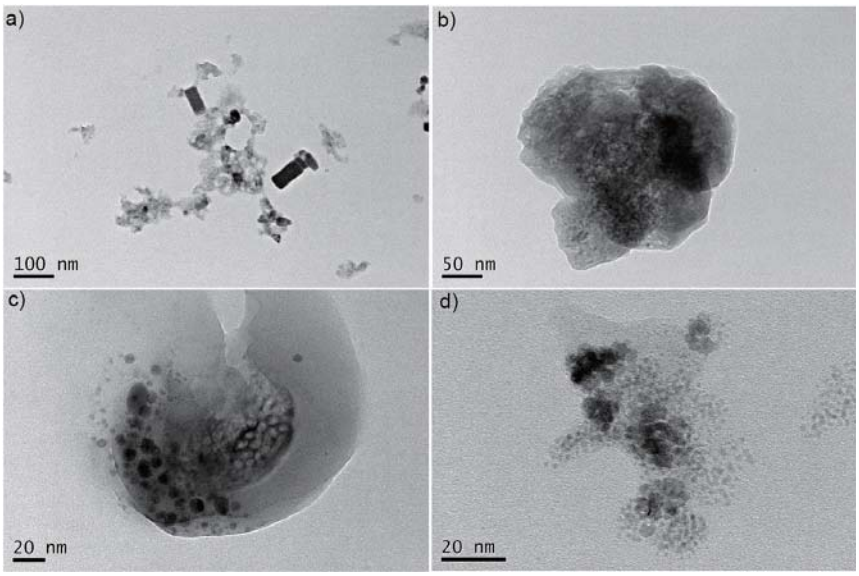

Fig. S8 TEM images of (a), (b), (c), and (d) Peptide-Pt without RGOs hybrids.

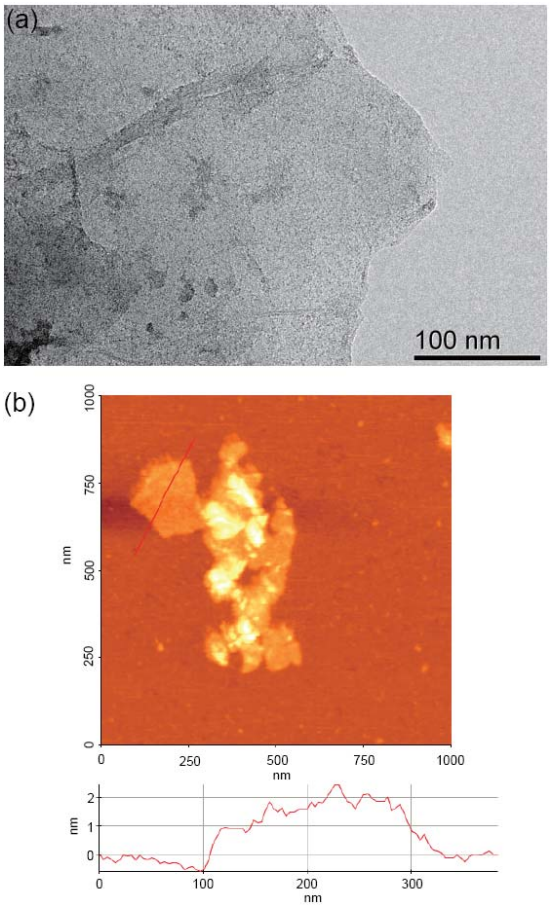

Fig. S9 TEM image of RGOPN-Pt and (b) AFM image of RGOPN hybrids.

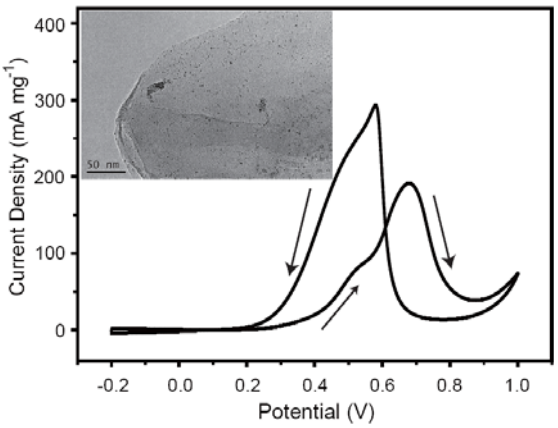

Fig. S10 CV curve of RGOPN-Pt catalysts measured in electrolytes of 0.5 M H_2SO_4 and 1.0 M CH_3OH at a scan rate of 50 mV s^{-1} and Inset is TEM image of RGOPN-Pt catalyst after 30 cycle scans.

Table S1 Analysis of the deconvoluted C 1s peaks and their relative atomic percentage from XPS for RGOPN and RGOP hybrids.

	C 1s fitting binding energy (eV; relative atomic percentage, %)			
Sample	C–C	C–O/C–N	C=O	N–C=O
RGOPN	285 (78.51)	285.7 (4.96)	287.05 (11.17)	288 (5.36)
RGOP	285 (67.8)	285.7 (12.14)	287.05 (9.64)	288 (10.42)